*PHYSOR 2010 – Advances in Reactor Physics to Power the Nuclear Renaissance*
Pittsburgh, Pennsylvania, USA, May 9-14, 2010, on CD-ROM, American Nuclear Society, LaGrange Park, IL (2010)

# HTTR FUEL BLOCK SIMULATIONS WITH SCALE

**Dan Ilas, Jess Gehin**
Oak Ridge National Laboratory
P.O. Box 2008, Oak Ridge, TN 37831-6170
ilasd@ornl.gov

## ABSTRACT

The SCALE code system is currently being updated to improve the methods and data to support High Temperature Gas Cooled reactor analysis. This paper presents the results of a High Temperature Engineering Test Reactor (HTTR) fuel block analysis with SCALE6.0, which is included as one of the sources of validation data. Good agreement is reported between continuous energy and multigroup SCALE/KENO models of the HTTR block for eigenvalue and fission density distribution. The agreement of the SCALE/KENO results with the MCNP5 results is also very good. The boundary condition is shown to have a large effect on both the calculated eigenvalue and the fission density distribution within the fuel block. In addition to the reported results, a method is proposed to alleviate the fuel mass non-conservation due to the clipping of the lattice of grains within the fuel element in the Monte Carlo continuous energy models.

*Key Words*: NGNP, HTGR, eigenvalue, fission density

## 1. INTRODUCTION

One of the high-temperature gas-cooled (HTGR) reactor technology options under consideration by the Next Generation Nuclear Plant (NGNP) project is based on the prismatic, graphite-moderated reactor design [1]. Within this context, the capability to generate accurate three-dimensional (3-D) core power distributions is one of the main challenges for the NGNP methods development.

The current neutronic computational methodology for core power mapping was developed primarily for light water reactors (LWRs) and is based on two-dimensional (2-D) transport calculations at the assembly level to generate nodal parameters, followed by 3-D diffusion-based calculations at the core level. To extend this methodology to the new NGNP designs, additional detailed testing is necessary to ensure that the critical parameters are accurately calculated. To respond to these requirements, a project is under way at Oak Ridge National Laboratory (ORNL) to investigate and evaluate HTGR reactor physics issues and develop an understanding of the key behavior of pebble-bed and prismatic HTGRs. Existing codes and models will be assessed by using available experimental data and by comparisons with other codes. The study presented in this paper, along with another study on pebble-bed reactor configurations [2], addresses a few of the issues considered to be important in the understanding of HTGR modeling.

The available experimental data necessary to benchmark the current computational methods on prismatic designs are currently limited. One such set of experimental data is provided by startup measurements on the High Temperature Engineering Test Reactor (HTTR) [3]. This 30 MWth, prismatic design, graphite-moderated, helium-cooled reactor was built by the Japan Atomic Energy Agency (JAEA), with the first criticality achieved with an annular core on November 10, 1998, and with the full-core criticality attained on December 16, 1998. The core of this reactor consists of fuel blocks with different fuel enrichments of up to 10 wt%. These blocks are arranged in five-block columns that are intermixed with control rod

columns and surrounded by reflector blocks. The fuel blocks are regular hexagonal prisms with a height of 58 cm and an apothem of 18 cm. Each fuel block contains either 31 or 33 fuel pins of constant enrichment arranged in a triangular pitch and two burnable poison (BP) pins in two corners of the hexagon at 120° with respect to the center of the hexagon. One characteristic of the fuel pins that distinguishes them from the proposed NGNP design is their annular shape. The fuel is made of TRISO (tri-isotropic) particles with a $UO_2$ kernel and embedded in a graphite matrix in the form of an annular cylinder.

This study focuses on the 3-D modeling of an HTTR fuel block with the SCALE code system [4]. Calculations have been performed with ENDF/B-VII multigroup cross sections (MG) processed with the "double heterogeneity" option and with continuous energy (CE) ENDF/B-VII cross section data. The multiplication constant and the fission density distributions have been analyzed and compared to the results obtained with the MCNP5 code [5]. In the context of this paper, "fission density" is in fact the fission neutron source density, i.e., the $\nu\Sigma_f$ reaction rate. It is shown that the magnitude of the axial heterogeneity is comparable to the radial-azimuthal one. By comparing the results obtained with reflective boundary conditions (commonly used in LWR calculations) to those obtained by using a periodic boundary condition, we show the importance of using the correct environment (boundary condition) for fuel block calculations.

## 2. HTTR FUEL BLOCK DESCRIPTION

The fuel block analyzed in this paper contains 33 pins, with the fuel kernels at 6.3% enrichment and the burnable poison (BP) rods with 2.5% $^{10}B$ content, based on the specifications provided in reference [3]. Figure 1 shows cross-sectional (Fig. 1a) and vertical (Fig. 1b) views of the fuel block considered. Each annular fuel pin (with an inner radius of 0.5 cm, an outer radius of 1.3 cm, a height of 54.6 cm, and a pitch between pins of 5.15 cm) is made of 14 fuel compacts, each 3.9 cm in height. The $UO_2$ fuel pins are enclosed in a graphite sleeve outside of which helium is circulated. The annular fuel pin contains 12987 TRISO fuel particles (Fig. 1c) embedded in a graphite matrix for a total mass of 188.58 grams of uranium. The TRISO grain is made of a spherical 0.03 cm-radius fuel kernel surrounded by four layers of carbon or silicon carbide.

The BP pin consists of two 20 cm long sections of absorber material at the top and bottom separated by a 10 cm thick section made of graphite discs. Only two of the three available BP positions in the fuel block are filled with the boron pin, the third one being left empty. A hole is provided at the center of the fuel block for handling purposes. Detailed material description and additional geometry details are given in reference [3].

For use in this paper, the locations of the fuel and BP pins in the cross-sectional view of the fuel block will be numbered using the format *mn*, with *m* identifying the row from the bottom to the top on Fig. 1a and *n* the position on the row from left to right (e.g., "11" will identify the BP pin in the lower left corner, "12" the fuel pin to its right, and "44" the handling hole, while "47" will be the empty BP location).

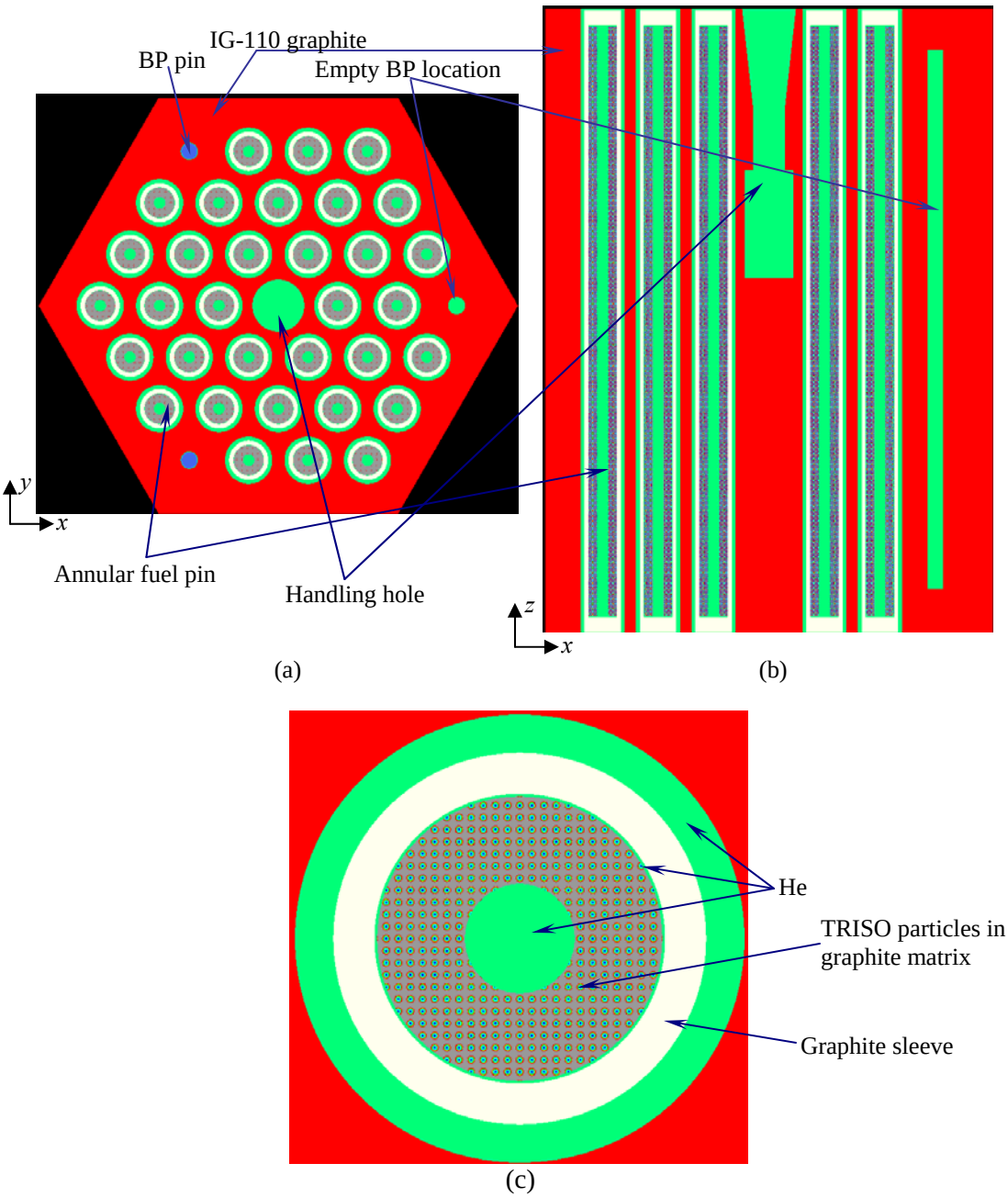


**Figure 1. Cross-sectional (a), vertical (b) views of the HTTR fuel block and fuel pin detail with explicit TRISO particles modeling (c) for the SCALE/KENO CE model**

## 3. TRISO PARTICLE MODELING

One important feature of the HTGR fuel block design is the double spatial heterogeneity. The first level of heterogeneity is provided by the distribution of the TRISO grains inside the fuel compact, while the second level is given by the lattice of fuel pins in the fuel block.

In modeling the first level of heterogeneity, the parameter that primarily needs to be conserved is the amount of fuel per fuel pin, which is set to 188.58 ± 5.66 g uranium for fresh HTTR fuel. The density of the fuel kernel is 10.39 g/cm$^3$. One way to conserve this mass is to fully include the lattice of fuel grains within the fuel pin. In using this approach, however, the lattice must have a smaller pitch to avoid the clipping of the TRISO particles at the boundaries of the fuel pin. This will create a different spatial distribution (non-physical local packing fraction) of the TRISO particles, with the regions near the boundaries of the pin containing no TRISO particles. A rigorous random placement (not based on a lattice) of the individual TRISO particles within the fuel pin that also preserves the mass of fuel can be imagined and has been previously demonstrated [6]. However, because the number of TRISO particles is very large (~5 million per fuel block in this case) this modeling approach is only (computationally) feasible for small configurations (e.g., single fuel compact). Also, the rigorous analytical total fuel mass (or, equivalently, volume) calculation necessary to assess the fuel mass conservation is nontrivial when clipping is allowed. In both SCALE/KENO and MCNP a statistical approach based on Monte-Carlo integration can be used to calculate the total volume, but this approach can lead to relatively large uncertainties. For example, the usage of one billion random points in SCALE/KENO to statistically calculate the fuel volume leads to differences greater than 2% between the estimations of the fuel volume for different compacts (these volumes should be identical).

Given the above arguments, an alternative approach is proposed in this paper that is conjectured to conserve the mass in a statistical sense, while also preserving the uniform spatial distribution. It is important to note first that the MG approach in SCALE's 3-D Monte Carlo transport code KENO uses a "double-heterogeneous" treatment [7] to account for resonance self-shielding effects. In this approach both the mass of fuel and its uniform spatial distribution are rigorously preserved.

In the CE approaches in SCALE/KENO and in MCNP, the TRISO particles can be modeled exactly and placed in a lattice that is embedded in the fuel pin. The lattice pitch can be precisely determined from the mass conservation condition when the type of lattice (e.g., "simple cubic") is imposed. When the lattice of grains is placed in the fuel pin, clipping can appear that can lead to a slight non-conservation of the mass. If the lattice is shifted by a random vector, the clipping will also be random. Consequently, if this random shift is repeated multiple times, we assert that on average the fuel mass will be conserved, while also preserving the uniform distribution of grains in the matrix. It was calculated that the error in the total volume for TRISO kernels can be as large as 1% for an annular pin as a result of fuel particle clipping, but if the lattice of fuel kernels is randomly shifted, the error in the mean calculated volume decreases significantly (e.g., for 1 million realizations this error was ~$10^{-6}$ for a configuration close to a fuel pin used in this study). In MCNP this technique can be implemented by using the URAN card and running multiple instances with different seeds for the random number generator. Table I shows four values of the multiplication constant obtained for the HTTR fuel block of Fig. 1 (reflective boundary conditions) with four different seeds for the random number generator and using otherwise identical input files. For the SCALE/KENO simulation, the lattice was shifted by a random vector with components smaller than half the size of the lattice pitch. The results for four such cases are summarized in Table II. As can be observed from either Table I or II, the difference between individual cases can be as large as 58 pcm for the cases analyzed, but differences of 100 pcm or larger have been observed for other configurations. If the four cases are interpreted statistically, an average value can be calculated that is believed to better represent reality. When this is done, an additional error, due to mass non-conservation, must be added to the statistical standard variation. The last column on the "*Average*" rows in Tables I and II shows the estimate of the standard deviation due to mass non-conservation, calculated from the four runs above ($N$=4) as shown in Eq. 1 below.

$$\sigma^{m}_{k_{eff}} \equiv \frac{1}{N}\sqrt{\sum_{i=1}^{N}\left(k_{eff,i} - \bar{k}_{eff}\right)^2} \qquad (1)$$

The statistical error of the average was calculated considering the four cases as uncorrelated.

**Table I. MCNP5 distribution of the multiplication constants for four cases using different seeds**

| Seed # | $k_{eff}$ | *Statistical* $\sigma_k$ | $k_{eff} - \bar{k}_{eff}$ |
|---|---|---|---|
| **1** | 1.33034 | 0.00024 | -0.00028 |
| **2** | 1.33077 | 0.00026 | +0.00015 |
| **3** | 1.33054 | 0.00024 | -0.00008 |
| **4** | 1.33084 | 0.00023 | +0.00022 |
| ***Average*** ($\bar{k}_{eff}$) | 1.33062 | 0.00012 | 0.00010 |

**Table II. SCALE/KENO-VI distribution of the multiplication constants for four cases using randomly shifted lattice**

| Case # | $k_{eff}$ | *Statistical* $\sigma_k$ | $k_{eff} - \bar{k}_{eff}$ |
|---|---|---|---|
| **1** | 1.33186 | 0.00027 | +0.00040 |
| **2** | 1.33138 | 0.00030 | -0.00008 |
| **3** | 1.33128 | 0.00033 | -0.00018 |
| **4** | 1.33131 | 0.00029 | -0.00015 |
| ***Average*** ($\bar{k}_{eff}$) | 1.33146 | 0.00015 | 0.00012 |

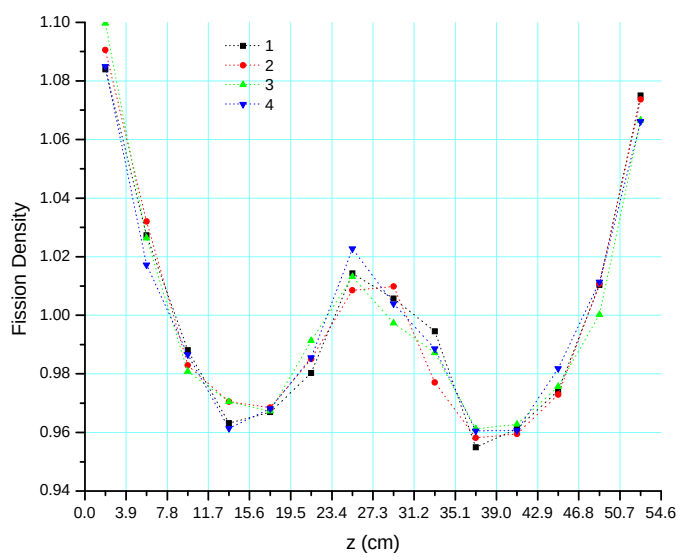


**Figure 2. Axial fission density distribution in pin 12 of the HTTR fuel block for four cases using randomly shifted lattice**

The axial fission density distribution for pin 12 (normalized to the average fission density per compact) is shown in Fig. 2. The results were obtained with SCALE/KENO-VI in CE mode for the same four random shifts of the lattice. Variations of ~2% (significantly larger than the statistical errors in scalar fluxes,

which are smaller than 0.1% for the pin thermal flux) can be observed for both the axial and the *x-y* shapes of the 3-D fission density distribution.

## 4. SIMULATIONS RESULTS AND DISCUSSIONS

The simulations and the comparisons described below are based on consistent single configurations and do not use any averaging based on the randomly shifted lattice approach described in the previous section for SCALE/KENO and MCNP5 calculations. ENDF/B-VII cross-section libraries were used in both the MCNP and SCALE/KENO simulations.

### 4.1. Multiplication Constant Comparisons

The configuration in Fig. 1 was modeled in SCALE/KENO with the CE option and in MCNP5 without using the URAN card. Because the double-heterogeneity procedure for cross-section processing does not support annular pins at this time, the annular fuel was homogenized with the central hole to form a solid cylindrical pin for the MG option in SCALE/KENO. The MG option is the one currently used in SCALE codes for sensitivity/uncertainty analysis and for depletion calculations. A similar procedure was then used with the CE option of SCALE/KENO (case 4 in Table III) to assess the error introduced by this homogenization.

Table III shows the multiplication constant obtained in each case. The value for SCALE/KENO CE is the same as the first value listed in Table II, which is considered as reference. These reference cases correspond to the case with no shift in SCALE/KENO, respectively to the default seed value and no URAN card in MCNP. From the comparison between cases 1 and 3, it turns out that the SCALE/KENO-VI CE and MCNP5 have an excellent agreement. The eigenvalue predicted by the SCALE/KENO-VI CE model is 85 ± 35 pcm higher than the MCNP5 result. The difference between the averages of Table I and II is 84 ± 19 pcm (only statistical standard deviation included as uncertainty). The multigroup result is 336 ± 37 pcm lower than the continuous energy SCALE/KENO result. As observed from cases 1 and 4, the homogenization of the fuel pins with their central holes leads to an overestimation of the result by 68 ± 37 pcm. When the eigenvalue of case 4 is compared to the average eigenvalue calculated in Table II, however, the difference is 108 ± 30 pcm. We conclude that, although small, the error introduced by the homogenization of the central hole into the fuel pin is statistically significant. The axial homogenization of the central handling hole has virtually no effect on the multiplication constant, as observed for case 5 in Table III.

The last column of Table III shows the CPU time for each calculation. The MCNP5 code used the OpenMPI-compiled parallel version. Both the SCALE/KENO and the MCNP5 simulated 11 million particles, i.e. 110 generations (cycles), 10 skipped, 100,000 particles per generation cycle. From Table III the MG version of SCALE/KENO is over three times faster than the CE version for the same number of particles simulated.

Calculations for cases 1 through 5 were performed using reflective boundary conditions, in accordance with the current lattice level methodology for light water reactors. The application of a white boundary condition (results not shown) has virtually no effect on the multiplication constant. The use of a periodic boundary condition (case 6), however, seems to have a relatively large effect; the multiplication constant in this case is 861 ± 43 pcm lower than that for the case when a reflective boundary condition was used (case 2). This is due to the different virtual positions of the BP pins around the fuel block when the periodic boundary condition is used as opposed to the reflective boundary condition.

**Table III. Multiplication constants for different models**

| Case # | Description | $k_{eff}$ | $\sigma_k$ | *CPU time (hours)* |
|---|---|---|---|---|
| **1** | **SCALE/KENO-VI CE** | 1.33186 | 0.00027 | 14.00 |
| **2** | **SCALE/KENO-VI MG** | 1.32850 | 0.00025 | 4.29 |
| **3** | **MCNP5** | 1.33101 | 0.00024 | 142.47 |
| **4** | **SCALE/KENO-VI CE with homogenized pins** | 1.33254 | 0.00026 | 13.82 |
| **5** | **SCALE/KENO-VI CE with homogenized handling hole** | 1.33164 | 0.00022 | 14.01 |
| **6** | **SCALE/KENO-VI CE with periodic boundary conditions** | 1.32325 | 0.00033 | 14.03 |

## 4.2. Fission Density Distribution Comparisons

Pin fission density distributions were calculated using three models: (1) an MCNP5 model, (2) a SCALE/KENO-VI CE model, (3) and a SCALE/KENO-VI MG model. In all of these three cases, a reflective boundary condition was used.

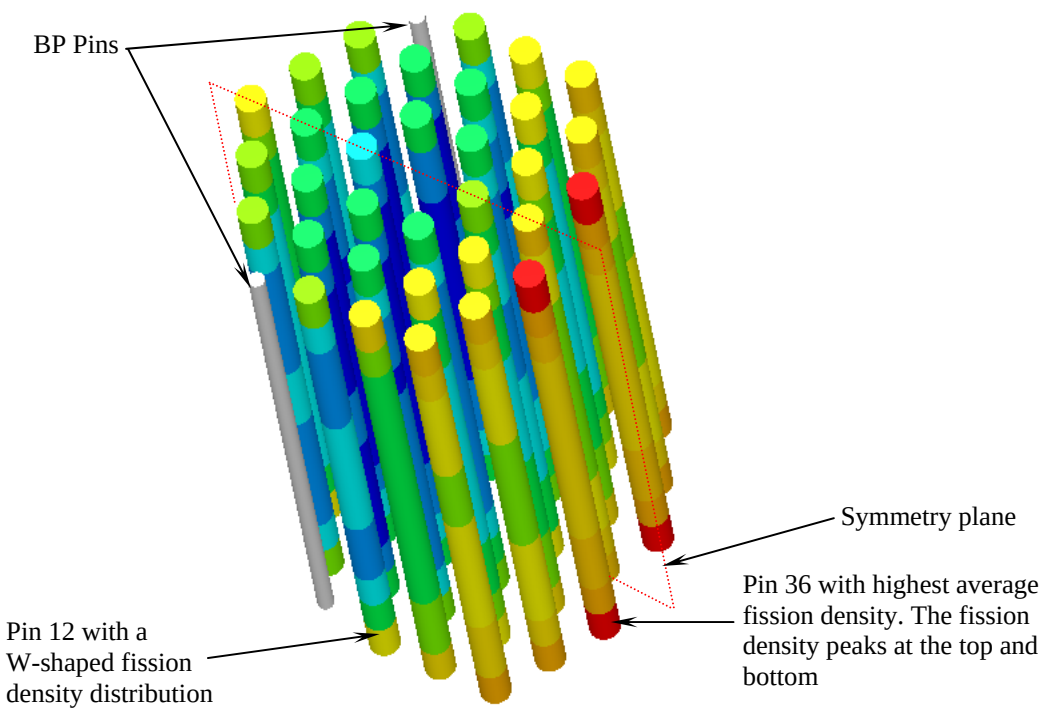


**Figure 3. Three-dimensional pin fission density distribution in the HTTR fuel block with SCALE/KENO MG.**

Figure 3, obtained with KENO3D, illustrates the 3-D distribution of the fission density in all 33 fuel pins as calculated by SCALE/KENO MG. Each axial zone corresponds to a fuel compact in which the fission

density was averaged. The color-coded values for fission density clearly suggest that the distribution peaks at the top and bottom of the pins furthest from the BP pins.

The radial-azimuthal distribution of the calculated fission density in each pin for each of the three models is illustrated in Fig. 4. The symmetry of the fuel block was taken into account to reduce the number of distinct pins from 33 to 19. In accord with the pin numbering convention introduced in section 3 each decade on the abscissa axis in Fig. 3 corresponds to a row of pins in Fig. 1a.

The three models listed above, all using the same reflective boundary condition, show excellent agreement. The differences are small, below 1% between their predictions for all the pins, and are hardly visible on the plot. The statistical errors are negligibly small (~0.1%) and are not shown. The fission density peaks in pin 36. It is interesting to notice the parabolic shape of the fission density distribution in each row of pins with the $R^2$ value of the parabolic fit for each row better than 0.99. Figure 4 shows the fitting parabolas for the SCALE/KENO CE values.

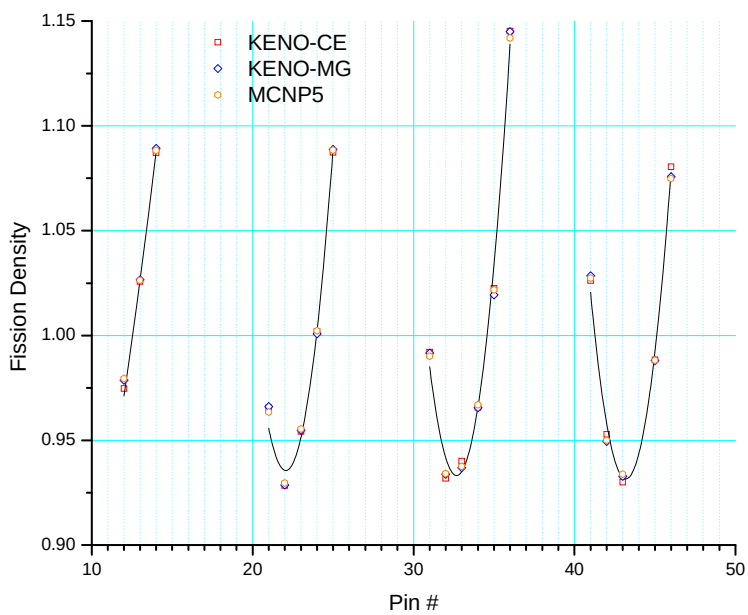


**Figure 4. Pin fission density distribution in the HTTR fuel block with three models.**

The axial fission density distribution takes a cosine shape with a minimum at the middle of the pin (as opposed to a LWR fission density distribution, which usually peaks at the middle) when the fuel pin is far from the BP pins but is “W” shaped for fuel pins near the BP pin as a result of the graphite region in the middle of the BP pins. Figure 5 shows such a “W” fission density distribution in pin12 (and pin 72) located near the BP pin. The same good agreement (differences no larger than 1%) between SCALE/KENO values and MCNP values can be observed axially.

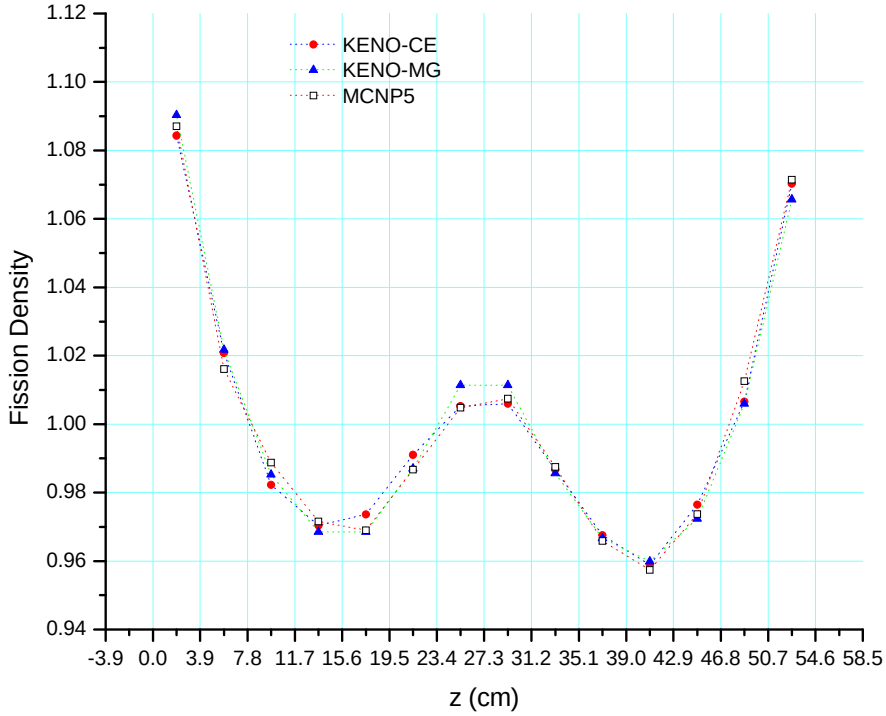


**Figure 5. Axial fission density distribution in pin 12 of the HTTR fuel block.**

As with the multiplication constant, the periodic boundary condition (results are not shown in Fig. 3) also changes the fission density distribution by a large amount: as much as 7% for pin 36, which is near the empty BP location. For the periodic boundary condition, the fission density has almost equal values in pins 13, 36, and 41. Also, this boundary conditions leads to a flatter pin fission density distribution throughout the fuel block. The large differences in fission density distribution, together with the large difference in the multiplication eigenvalue predicted with the periodic boundary condition, demonstrate the importance of using the correct boundary conditions for the fuel block calculations.

## 5. CONCLUSIONS

An HTTR fuel block has been simulated in SCALE 6.0 using the 3-D Monte Carlo code KENO-VI and the ENDF/B-VII-based libraries (CE and MG). The results for pin fission density distributions show excellent agreement between the CE and the MG options in SCALE/KENO, and both agree very well with the results of the MCNP5 simulations. The differences observed were below 1%.

The multiplication constant results show excellent agreement between KENO-VI CE and MCNP5 with a difference of 85 ± 35 pcm. The difference between the CE and MG options in KENO is 336 ± 37 pcm. The pin homogenization necessary in the multigroup model of SCALE/KENO results in ~100 pcm effect in the eigenvalue.

It is shown that the boundary treatment for the fuel block is very important for both the multiplication constant and the fission density distribution. In particular, the multiplication constant calculated with the periodic boundary condition is almost 1% smaller than the one calculated with reflective boundary conditions.

In addition to the above comparisons and observations, a method was proposed and discussed to alleviate the possible fuel mass non-conservation due to the clipping of the grain lattice.

## 6. ACKNOWLEDGMENTS

This work was funded by the U.S. Nuclear Regulatory Commission through contract JCN N6842 on HTGR physics issues. Thanks are extended to Steve Bowman and Matt Jessee for comments during the internal review process. Mark Williams is acknowledged for recommendations on cross section processing in SCALE/KENO MG.

## REFERENCES

1. "Next Generation Nuclear Plant Methods Research and Development Technical Program Plan," http://www.inl.gov/technicalpublications/Documents/4196366.pdf , INL/EXT-06-11804 PLN-2498, Revision 1 (September 2008).
2. G. Ilas, "On SCALE Validation for PBR Analysis," submitted to *PHYSOR 2010*, Pittsburgh, PA, May 9–14, 2010.
3. J. D. Bess and N. Fujimoto, evaluators, "Evaluation of the Start-up Core Physics Tests at Japan's High Temperature Engineering Test Reactor (Fully-Loaded-Core)," HTTR-GCR-RESR-001, Revision 1, to be published in *International Handbook of Evaluated Reactor Physics Benchmark Experiments*.
4. *SCALE: A Modular Code System for Performing Standardized Computer Analyses for Licensing Evaluation,* ORNL/TM-2005/39, Version 6, Vols. I–III, Oak Ridge National Laboratory, Oak Ridge, TN (2009). (Available from Radiation Safety Information Computational Center at Oak Ridge National Laboratory as CCC-750.)
5. X-5 Monte Carlo Team, *MCNP—A General Monte Carlo N-Particle Transport Code, Version 5*, LA-CP-03-0245, Los Alamos National Laboratory, Los Alamos, NM (2003).
6. E. Bomboni, N. Cerullo and G. Lomonaco, "Analysis of Pebble-Fueled Zone Modeling Influence on High-Temperature Reactor Core Calculations", *Nuclear Science and Engineering*, **162**, pp.282-298 (2009).
7. M. L. Williams, S. Goluoglu, and L. M. Petrie, "Recent Enhancements to the SCALE 5 Resonance Self-Shielding Methodology," *ANS Transactions,* **92,** p. 751 (2005).